Journal of
Applied Research in Water and Wastewater
Journal homepage: www.arww.razi.ac.ir

Original paper

Numerical simulation of the effects of downstream obstacles on malpasset dam break pattern

Hamed Azimi[1], Majeid Heydari*[,2], Saeid Shabanlou[3]

[1]*Young Researchers Club, Kermanshah Branch, Islamic Azad University, Kermanshah, Iran.*
[2]*Department of Science and Water Engineering, Faculty of Agriculture, Bu-Ali Sina University, Hamedan, Iran.*
[3]*Department of Water Engineering, Kermanshah Branch, Islamic Azad University, Kermanshah, Iran.*

ARTICLE INFO

Article history:
Received 20 October 2018
Received in revised form 20 November 2018
Accepted 30 November 2018

Keywords:
Dam break
Malpasset dam
Numerical simulation
Flow pattern

ABSTRACT

Dam break is an important phenomenon which significantly affects the environment as well as the inhabitants of the downstream areas of the dam. In the present study, the hydraulic break of Malpasset dam as a result of sudden flooding was simulated numerically using the FLOW-3D software. The two-equation k-ε turbulence models and RNG k-ε turbulence model were used to simulate the flow field turbulence. Also, the free-surface variations of the flow were simulated using the VOF (Volume of Fluid) scheme. The results obtained from the numerical model were in good agreement with those predicted by the EDF model. Based on the simulation results, the maximum pressure occurred at the lower layers of the flow and reduced as the free surface of the flow was approached. The maximum pressure increased at each point in time. The maximum longitudinal velocity occurred at the front of the advancing wave resulting from break of the dam, and subsequently decreased due to the increasing depth at the downstream of the dam. Additionally, the effects of obstacles with different shapes on the flow pattern arising from dam break (due to sudden flooding) were also investigated. Examination of these effects revealed that the cubic obstacle placed obliquely in the flow direction produced the maximum separation region at its downstream. Conversely, this separation region was eliminated completely when a cylindrical obstacle was used. The maximum and minimum Froude numbers were obtained for the flow encountering the perpendicular cubic obstacle and the flow impacting the cylindrical obstacle, respectively.

1. Introduction

Dam break is an important consideration in the design of dams. If a dam collapses, a huge wave is containing mud, dam reservoir water and dam body materials starts moving, thus threatening the land, people, or residential areas that are located in its path. Numerous theoretical and experimental studies have been conducted regarding dam break. Bellos et al. (1992) performed a 2D laboratory experiment on dam break. Bell et al. (1992) conducted a research on one-dimensional and two-dimensional break of a dam using a channel with a 180-degree bend for the 2D break analysis, and compared the results obtained for various cases. Fraccarollo and Toro (1995) investigated the 2D break of a dam numerically and experimentally, and compared these results. Aziz Khan et al. (2000) studied dam break by taking into account the effect of suspended particles on the break wave and examined the velocity profile of the same via hexahedron particles, using mobile cameras along the channel to record their results. Soares and Zech (2002) studied dam break at bends where a 90-degree bend, a dry bed, and a rectangular channel were implemented to measure velocity and the free water surface during dam break. Using a 3D channel, Mirei and Akiyama (2003) investigated the effects of hydrodynamic forces during break on the structures located downstream of the dam. Bellos (2004) studied the 2D wave motion triggered by flooding in two different cases: dry bed and wet bed, and subsequently compared the obtained results. Bellos (2004) measured flow depth at various hydraulic conditions and recorded the hydrographs corresponding to different flooding conditions. Eaket et al. (2005) devised a new method for recording the results obtained from dam break via imaging and converting it into photographs which were subsequently used for producing the required results to determine the surface water profile. Cagatay and Kocaman (2011) conducted experimental and numerical studies on the flow resulting from flooding of water over the body of the dam. They compared their numerical results with those obtained from the experimental study. They used the FLOW-3D software for simulating their numerical model, and implemented the Navier-Stokes (RANS) and the SWE (Shallow Water Equation) equations to solve their flow field. In their study, Cagaty and Cocamen investigated the flow field and free surface profile resulting from water flooding over the dam. Kochman and Guzel (2011) studied, numerically and experimentally, the phenomenon of dam break and the resulting waves hitting downstream obstacles. They used the FLOW-3D for simulation. For solving numerically the flow field, they implemented the Reynolds-averaged Navier–Stokes (RANS) equations and for simulating flow field turbulence, they used the two-equation turbulence model. They also studied the damage caused by the break to the structures that were situated downstream of the dam. Using the equations for shallow waters (SWE), Singh et al. (2011) developed a 2D model for simulating Malpasset Dam break. Caboussat et al. (2012)

*Corresponding author Email: Heydari.majeid@gmail.com

developed a 3D model for simulating dam break flow and the consequent flooding by using the Reynolds averaged Navier-Stokes equations and the VOF (Volume of Fluid) scheme. Their 3D model was capable of taking into account the topographic effects at the break location. Caboussat et al. (2012) developed a numerical model for simulating the flooding that resulted from Malpasset Dam break. Using their own results, they also numerically simulated a hypothetical flooding situation that might have resulted from the break of Dixence Dam by considering the topography of the dam site. Developments in recent decades of computer software for numerically simulating of various phenomena has led to a considerable reduction in the expenses and the time spent for conducting experiments. In this study, the FLOW-3D software was used to simulate the break of Malpasset dam and its resulting break waves numerically. The numerical simulation of flow field turbulence was conducted via the two-equation and the RNG turbulence models. The VOF (Volume of Fluid) scheme was implemented for simulating the free surface variations of the flow.

Table 1. Specifications of the meshing used for measuring the sensitivity of the solution field.

Meshing	Cells along the x, y, and z axis
1	15×100×50
2	35×200×100
3	55×300×150
4	70×400×400

2. Materials and methods

2.1. Materials and instruments

Governing Equations

The continuity and the Reynolds-averaged Navier–Stokes equations were used for solving the incompressible fluid flow field:

$$V_F \frac{\partial \rho}{\partial t} + \frac{\partial(\rho u A_x)}{\partial x} + \frac{\partial(\rho v A_y)}{\partial y} + \frac{\partial(\rho w A_z)}{\partial z} = R_{SOR} \quad (1)$$

$$\frac{\partial u}{\partial t} + \frac{1}{V_F}\left(uA_x\frac{\partial u}{\partial x} + vA_y\frac{\partial u}{\partial y} + wA_z\frac{\partial u}{\partial z}\right) = -\frac{1}{\rho}\frac{\partial p}{\partial x} + G_x + f_x \quad (2)$$

$$\frac{\partial v}{\partial t} + \frac{1}{V_F}\left(uA_x\frac{\partial v}{\partial x} + vA_y\frac{\partial v}{\partial y} + wA_z\frac{\partial v}{\partial z}\right) = -\frac{1}{\rho}\frac{\partial p}{\partial y} + G_y + f_y \quad (3)$$

$$\frac{\partial w}{\partial t} + \frac{1}{V_F}\left(uA_x\frac{\partial w}{\partial x} + vA_y\frac{\partial w}{\partial y} + wA_z\frac{\partial w}{\partial z}\right) = -\frac{1}{\rho}\frac{\partial p}{\partial z} + G_z + f_z \quad (4)$$

where (u,v,w) , (A_x, A_y, A_z) , (G_x, G_y, G_z) and (f_x, f_y, f_z) respectively are speed component, fractional areas open to flow, gravitational force and accelerations resulted from viscosity along . Also, t, ρ, , , are time, fluid density, opening term, pressure and fractional volume open to flow respectively. The RNG turbulence model was used to simulate flow field turbulence. This model can simulate with high accuracy the turbulence of high-shear regions and low-intensity turbulent flows. Also, compared to the model, this two-equation turbulence model requires fewer empirical constants and shows a better performance when simulating separation regions. The VOF scheme was used for predicting the free surface variation of the flow. In this scheme, the following transfer equation was solved for calculating the partial-volume fluid:

$$\frac{\partial F}{\partial t} + \frac{1}{V_F}\left(\frac{\partial}{\partial x}(FuA_x) + \frac{\partial}{\partial y}(FvA_y) + \frac{\partial}{\partial z}(FwA_z)\right) = 0.0 \quad (5)$$

where, F is the partial volume of the fluid within a computational unit. If a certain computational unit is full of water, then F=1. F=0 represents the case where the cell is empty. If 0<F<1, then the cell contains both water and air [13].

Boundary Conditions

The boundary conditions for the numerical model were selected in accordance with the physical conditions of the Malpasset Dam. Since the dam collapsed as a result of flooding caused by rain and the consequent filling of the dam reservoir, forces arising from waves must be applied to the dam body at the upstream. Thus, with a given input wave, the wave amplitude and velocity, as well as the flow depth were determined at the inlet. These boundary conditions are equivalent to the wave boundary conditions in FLOW-3D. The solitary wave type was selected for the input wave to the Malpasset dam reservoir. All solid boundaries were defined as the Wall boundary conditions. The “No-slip” boundary condition was imposed on the wall and friction was neglected. Thus, no roughness is imposed at the wall boundary. The whole upper surface of the flow field was defined by the symmetry boundary condition. Under this type of boundary condition, frictions as well as temporal and spatial changes are zero for all parameters. At the downstream of the Malpasset dam, the outflow boundary condition was applied.

Flow Field Meshing

In simulating the Malpasset Dam break, the meshing within the whole computational range was implemented via a uniform block mesh consisting of rectangular elements. The sensitivity of numerical models to meshing has always been an important problem in numerical studies. Table 1 presents the specifications of the meshing implemented for break simulation of Malpasset Dam. The maximum water level in the EDF physical model measured by Electricit´e de France was used to verify the results obtained from the numerical model. Fig. 1 shows the maximum water level error obtained for various meshing. The maximum water level error predicted by the numerical model was considerably reduced with increasing number of computational cells. Fig. 2 shows the computational field meshing obtained from the FLOW-3D as well as various views of the meshing.

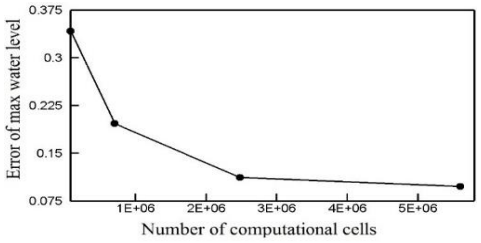

Fig. 1. Maximum water level error for different meshes.

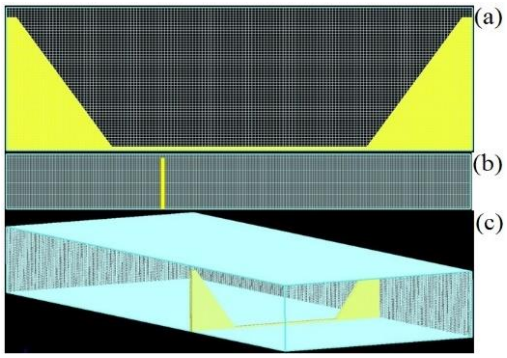

Fig. 2. Computational field meshing obtained from the FLOW-3D: a) transverse section, b) longitudinal section, c) 3D perspective.

Please cite this article as: H. Azimi, M. Heydari, S. Shabanlou, Numerical simulation of the effects of downstream obstacles on malpasset dam break pattern, Journal of Applied Research in Water and Wastewater, 5 (2), 2018, 441-446.

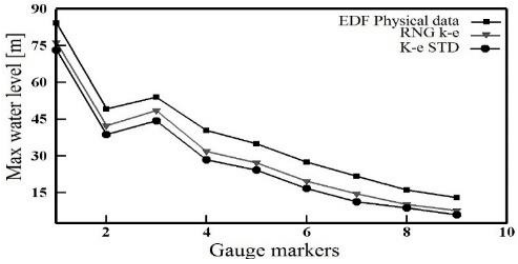

Fig. 3. Effect of standard and RNG turbulence models on maximum water level.

Effect of Turbulence Model on the Numerical Results

In this section, the effects of the two-equation turbulence model and the RNG model on hydraulic break patterns of Malpasset dam are investigated. The meshing and boundary conditions used here are set in accordance with the results obtained from the previous sections. In the standard turbulence model, two differential equations must be solved: the kinetic energy equation and the kinetic energy dissipation rate equation. The equations used in the RNG turbulence model, however, are similar to those used in the two-equation turbulence models (such as the standard model). These turbulence models are based on the Reynolds normalized groups which use statistical methods for obtaining an averaged equation for turbulence quantities. Models based on stress equations emphasize less on empirical parameters. The RNG turbulence model is an example of a turbulent model with a stress equation. However, the constants in this model are calculated explicitly, whereas those in the turbulence model are obtained empirically. Fig. 3 shows the effects of the standard k-ε turbulence model and the RNG model on the break pattern of Malpasset Dam. As can be seen, the RNG turbulence model provides a more exact simulation for maximum water height variations.

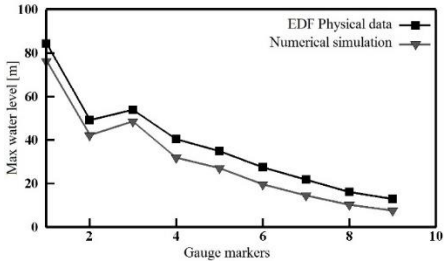

Fig. 4. Comparison of the results obtained for max water level form the numerical model and the EDF model.

Comparison of Simulation and EDF (Electricit´e de France) Results

The maximum water level values were obtained via the EDF (Electricit´e de France) physical model for verifying the numerical model and the simulation results obtained for the Malpasset dam break. Fig. 4 compares the results obtained from numerical simulation and those obtained from the physical model. Based on the simulation results, the numerical model predicted the max water level values with acceptable accuracy.

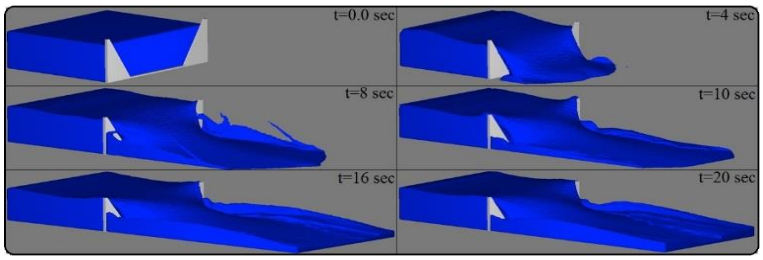

Fig. 5. 3D free surface variations of the flow at the instant of break.

3. Results and discussion

Fig. 5 shows the 3D flow free surface variation pattern at the instant the break occurred. As can be seen, at t=0.0, the water behind the dam is stable. Upon the breakage (break), a great volume of water is displaced from the reservoir towards the downstream areas of the dam. At t=4 sec, the wave resulting from the flooding enters the computational field and, in time, water engulfs the whole downstream of the dam structure.

Table 2. Geometrical properties of the obstacles used in numerical modeling.

Obstacle shape	Obstacle orientation	Obstacle Dimensions (m)
Cubic	Perpendicular to the flow direction	$40\times40\times40$ $(\text{length}\times\text{width}\times\text{height})$
Cubic	Oblique	$40\times40\times40$ $(\text{length}\times\text{width}\times\text{height})$
Cylindrical	_	40×40 $(\text{diameter}\times\text{height})$

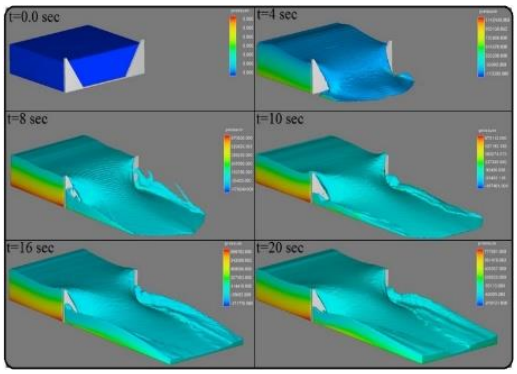

Fig. 6. Flow field pressure variations during break of the dam.

Pressure pattern as well as the minimum and maximum pressure values is important hydraulic parameters in the break pattern of a dam. In this section, pressure variations of Malpasset dam during its break are evaluated. Fig. 6 shows the pressure variations in the flow field during break of the dam. The simulation results show that the maximum pressure occurs at the lower layers of the flow and the pressure decreases towards the free surface. As time passes, the maximum pressure at each section in time increases.

During collapse of a dam, it is possible that supercritical and subcritical flows occur. Fig. 7 shows the Froude number variations during Malpasset dam collapse as well as the flow regime divisions. As can be seen in this figure, the flow undergoes supercritical conditions downstream of the dam body. A supercritical flow, due to its high energy, can cause extensive scouring and erosion. As can be seen, due to the great depth of the flow, the flow regime inside the reservoir is subcritical.

Please cite this article as: H. Azimi, M. Heydari, S. Shabanlou, Numerical simulation of the effects of downstream obstacles on malpasset dam break pattern, Journal of Applied Research in Water and Wastewater, 5 (2), 2018, 441-446.

Fig. 8 shows the longitudinal velocity component variations of the flow. It can be seen that the maximum longitudinal velocity occurs at the front of the advancing wave which results from the collapse of the dam, and subsequently, this velocity component decreases due to the increased flow depth downstream of the dam.

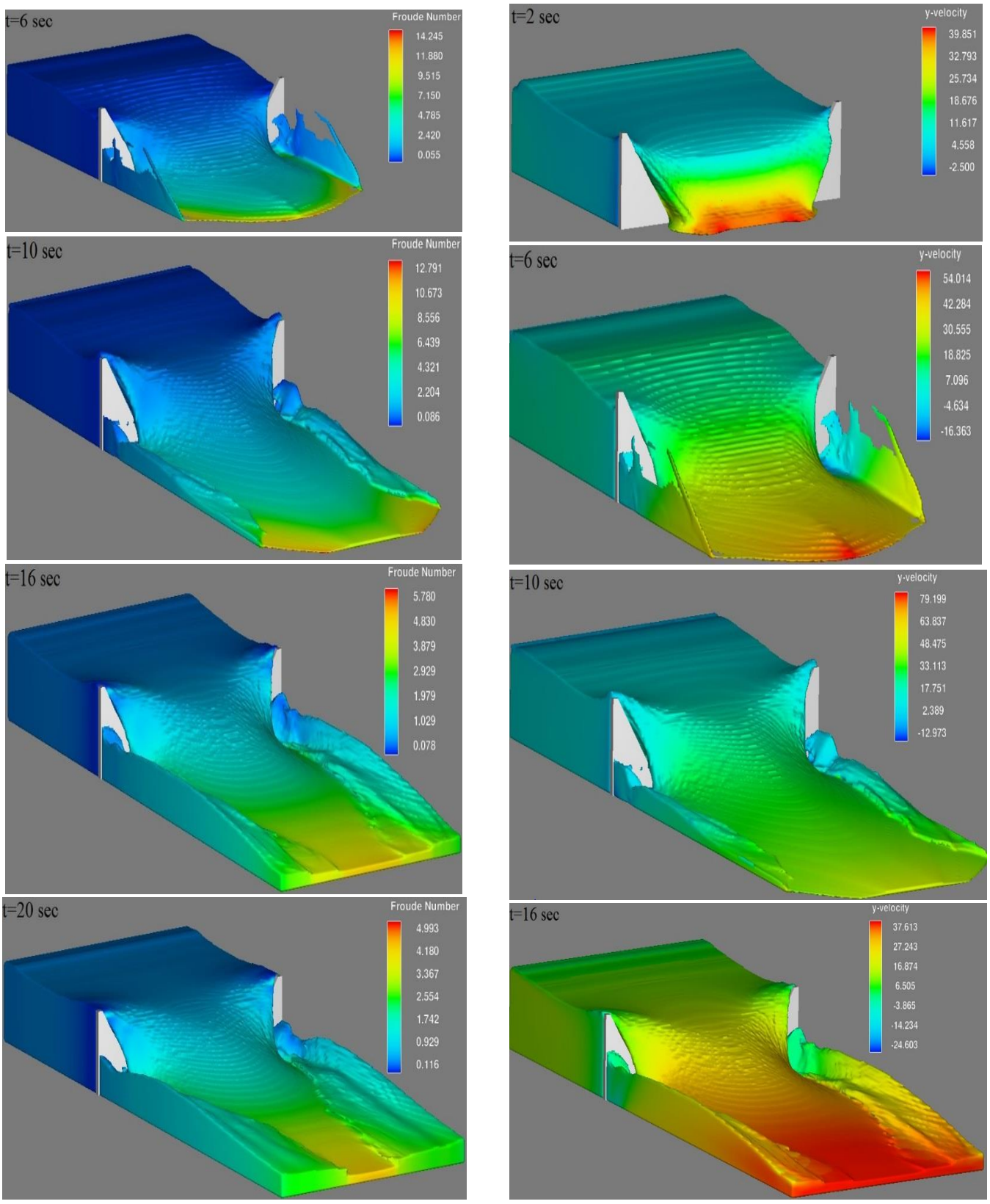

Fig. 7. Froude number variation pattern during the collapse of Malpasset dam.

Please cite this article as: H. Azimi, M. Heydari, S. Shabanlou, Numerical simulation of the effects of downstream obstacles on malpasset dam break pattern, Journal of Applied Research in Water and Wastewater, 5 (2), 2018, 441-446.

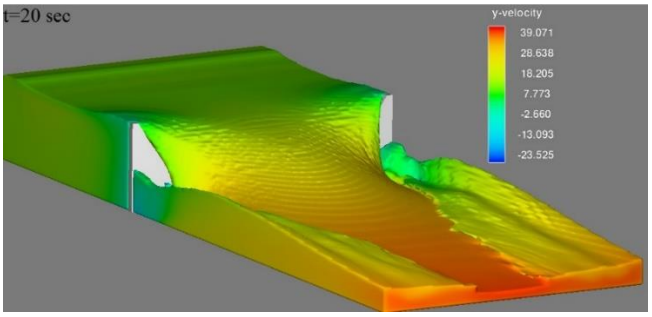

Fig. 8. Longitudinal velocity variations of the flow during collapse of Malpasset dam.

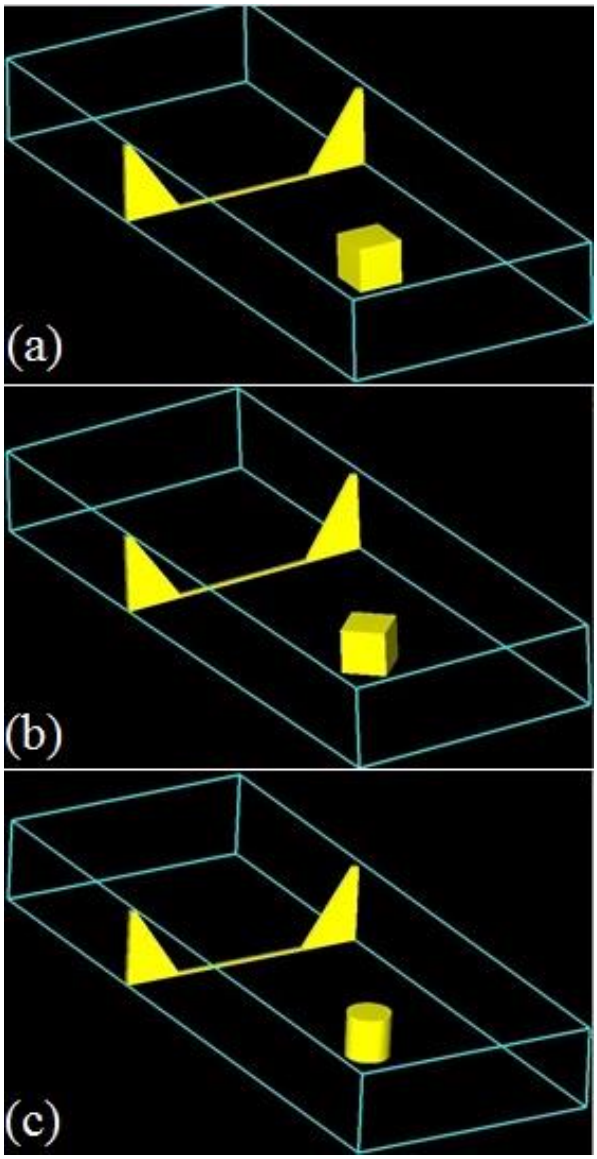

Fig. 9. Various obstacles with different shapes positioned downstream of the dam: (a) cubic obstacle perpendicular to the flow direction (b) oblique cubic obstacle (c) cylindrical obstacle.

3.2. Effect of Downstream Obstacles on the Flow Pattern during Collapse of Malpasset Dam

Dam breakage due to concurrent forces exerted on its reservoir as a result of flooding causes severe and irreparable damage to the lands and inhabitants of the areas downstream of the dam. In this study, the flow patterns during the collapse of Malpasset dam as various obstacles were encountered downstream of the dam structure were investigated. Table 2 shows the geometrical properties of the obstacles used in the numerical modeling. Fig. 9 shows the schematic of the flow field along with variously-shaped obstacles.

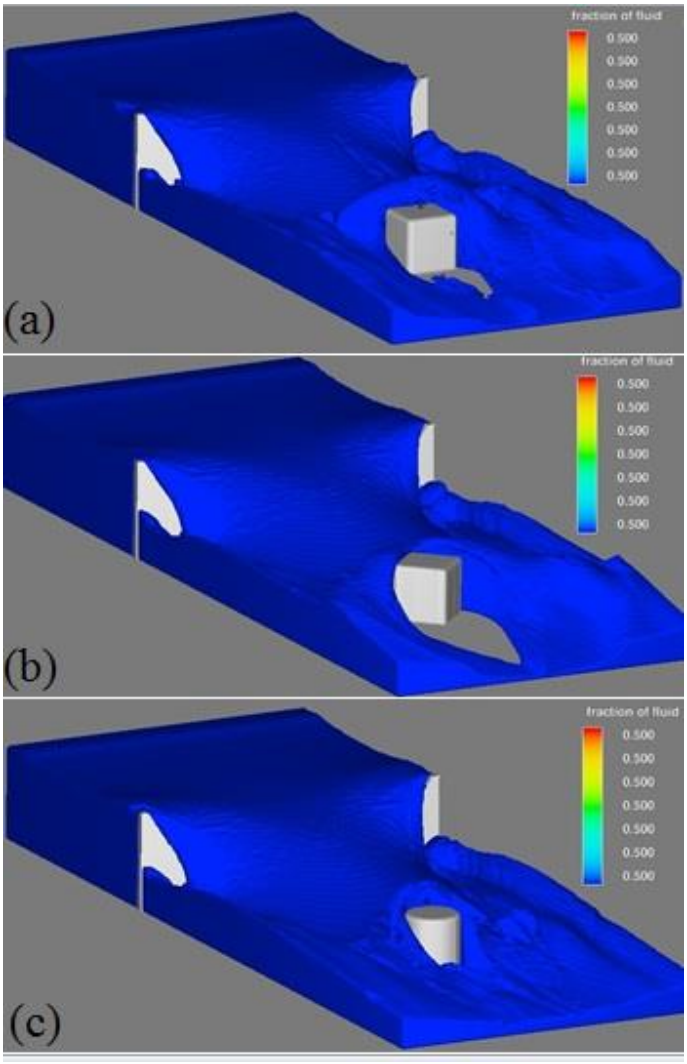

Fig. 10. 3D free surface variation patterns obtained as the flow encountered obstacles with different shapes: (a) cubic obstacle perpendicular to the flow (b) oblique cubic obstacle (c) cylindrical obstacle.

Fig. 10 shows the 3D free surface pattern of the flow as obstacles with different shapes are encountered. As can be seen, the greatest separation region occurs after the flow encounters Obstacle (b), i.e., the cubic oblique obstacle. Upon encountering Obstacle (c), however, no separation is observed due to the cylindrical shape of this obstacle.

The effects of obstacles shape on the Froude number after the dam break are shown in Fig. 11. As can be observed, the maximum Froude number at the downstream is obtained for cubic obstacle perpendicular to the flow direction. The minimum Froude number corresponds to the flow's impact with the cylindrical obstacle.

The longitudinal velocity component variations upon impact with obstacles having different shapes are shown in Fig. 12. Based on the simulation results, the maximum longitudinal velocity component is obtained for the perpendicular cubic obstacle. The variations of the longitudinal velocity component for the other two obstacles (i.e., oblique cubic and cylindrical) are similar.

4. Conclusions

Sudden unpredictable flooding of a dam reservoir is an important cause of dam break. Dam break is among the most significant hydrological and hydraulic phenomena which cause considerable damage to lands and inhabitants at the downstream of the dam. In this study, the break of Malpasset Dam and its resulting waves were

Please cite this article as: H. Azimi, M. Heydari, S. Shabanlou, Numerical simulation of the effects of downstream obstacles on malpasset dam break pattern, Journal of Applied Research in Water and Wastewater, 5 (2), 2018, 441-446.

numerically modeled by using the FLOW-3D. The flow field turbulence was modeled using the two-equation $k-\varepsilon$ and the RNG $k-\varepsilon$ turbulence models. Also, the variations of the free flow surface were simulated through the VOF scheme. As compared with the two-equation turbulence model, the RNG $k-\varepsilon$ model predicted the dam break pattern resulting from sudden flooding more accurately (based on the comparisons made with the results from the physical EDF model related to the break of Malpasset Dam). The 3D simulation by the RNG $k-\varepsilon$ model of the EDF physical model produced acceptable results. The simulation results showed that:

- Maximum pressure had occurred at the lower layers of the flow and that as the free surface of the flow was reached, the pressure decreased.

- The maximum pressure at each specific point in time would increase with time.

- The flow after the dam structure was supercritical which has high velocity and energy levels as well as high erosive and undermining power.

- Conversely, due to the great depth of the flow inside the reservoir, the flow regime inside the reservoir was subcritical.

- The maximum longitudinal velocity occurred at the front of the advancing wave resulting from dam break. This velocity component subsequently decreased as the flow depth increased downstream the dam.

- The greatest separation region occurred after the flow impacted the cubic oblique obstacle. The separation region was completely eliminated when the flow encountered the cylindrical obstacle.

- The maximum Froude number at the downstream of the dam was obtained for the perpendicular cubic obstacle and the minimum Froude number for the cylindrical obstacle.

- Based on the simulation results, the maximum longitudinal velocity occurred when the cubic oblique obstacle was placed in the path of the flow. The longitudinal velocity component variations were similar for the cubic oblique and the cylindrical obstacles.

Nomenclature

A_x, A_y, A_z	Fractional areas open to flow $\left(\mathrm{m}^2\right)$
F	Fluid volume fraction in a cell $(-)$
f_x,f_y,f_z	Viscous accelerations (m s^{-2})
G_x,G_y,G_z	Body accelerations (m s^{-2})
P	Pressure (N m^{-2})
R_{SOR}	Mass source $(-)$
T	Time (s)
u,v,w	Velocity components (m s^{-1})
V_F	Fractional volume open to flow $(-)$
x, y, z	Cartesian coordinate directions (m)
ρ	Fluid density (kg m^{-3})

References

Aziz khan A., Steffler P.M., Gerard R., Dam break with surges with floating debris, Journal of Hydraulic Engineering ASCE, 126 (2000) 375-379.

Bellos C.V., Experimental measurement of flood wave created by a dam break, European Water 7 (2004) 3-15.

Bellos C.V., Soulis J.V. and Sakkas J.G., Experimental investigation of two dimensional dam-break induced flows, Journal of Hydraulic Research 33 (1992) 843-864.

Bell S.W., Elliot R.C. and Chaudhry M.h., Experimental results of two dimensional dam-break flows, Journal of Hydraulic Research 30 (1992) 47-63.

Caboussat A., Boyaval S., Masserey A., Three-dimensional simulation of dam break flows, Mathicse Technical Report (2012)1-24.

Cagatay H.O, Kocaman S., Dam-break flow in the presence of obstacle: experiment and CFD simulation, Engineering Applications of Computational Fluid Mechanics 5 (2011) 41–552.

Eaket J., Hicks F.E., Peterson A.E., Use of stereoscopy for dam break flow measurement, Journal of Hydraulic Engineering ASCE, 131 (2005) 24-29.

FLOW 3D User's Manual. 2011. Version 10.0. Flow Science Inc.

Fraccarollo L., and Toro E.F., Experimental and numerical assessment of the shallow water model for two dimensional dam-break type problems, Journal of Hydraulic Research 33 (1995) 843-864.

Kocaman S., and Güzel H., Numerical and experimental investigation of dam break wave on a single building situated downstream. International Balkans Conference on Challenges of Civil Engineering, bcce, EPOKA University, Tirana, Albania, 2011.

Mirei Shige E., and Akiyama J., Numerical and experimental study of two-dimensional flood flows with and without structures, Journal of Hydraulic Engineering 129 (2003) 817-821.

Soares Frazao S., and Zech Y., Dam break in channels with 90 Bend, Journal of Hydraulic Engineering 128 (2002) 956-968.

Singh J., Altinakar M.S., Ding Y., Two-dimensional numerical modeling of dam break flows over natural terrain using a central explicit scheme, Advances in Water Resources 34 (2011) 1366-1375.

Please cite this article as: H. Azimi, M. Heydari, S. Shabanlou, Numerical simulation of the effects of downstream obstacles on malpasset dam break pattern, Journal of Applied Research in Water and Wastewater, 5 (2), 2018, 441-446.